



Published in final edited form as:

Geophys Res Lett. 2016 February 28; 43(4): 1710–1717. doi:10.1002/2016GL067841.

Spatiotemporal patterns and trends of Indian monsoonal rainfall extremes

Nishant Malik^{1,2}, Bodo Bookhagen³, and Peter J. Mucha¹

¹Carolina Center for Interdisciplinary Applied Mathematics, Department of Mathematics, CB #3250, University of North Carolina, Chapel Hill, NC 27599, USA

²Department of Mathematics, Dartmouth College, Hanover, NH 03755, USA

³Institute of Earth and Environmental Science, University of Potsdam, Karl-Liebknecht-Str. 24–25, 14467 Potsdam-Golm, Germany

Abstract

In this study, we provide a comprehensive analysis of trends in the extremes during the Indian summer monsoon (ISM) months (June to September) at different temporal and spatial scales. Our goal is to identify and quantify spatiotemporal patterns and trends that have emerged during the recent decades and may be associated with changing climatic conditions. Our analysis primarily relies on quantile regression that avoids making any subjective choices on spatial, temporal, or intensity pattern of extreme rainfall events. Our analysis divides the Indian monsoon region into climatic compartments that show different and partly opposing trends. These include strong trends towards intensified droughts in Northwest India, parts of Peninsular India, and Myanmar; in contrast, parts of Pakistan, Northwest Himalaya, and Central India show increased extreme daily rain intensity leading to higher flood vulnerability. Our analysis helps explain previously contradicting results of trends in average ISM rainfall.

1. Introduction

Large parts of South Asia and Southeast Asia receive more than 80% of their annual rainfall during the four summer months of June, July, August and September (JJAS) [*Bookhagen and Burbank*, 2010] (see Fig. S1). The strong rainfall seasonality is caused by the Indian Summer Monsoon (ISM) system and is a critical climatic phenomenon for over a billion inhabitants of the South and Southeast Asian region, with significant socio-economic impacts. Much of the cultural, economic, and agricultural life centers around the ISM season in this densely-populated region of the world [*Webster et al.*, 1998a; *Gadgil and Gadgil*, 2006; *Gadgil and Kumar*, 2006].

Despite the ISM's significance, there still remain large uncertainties about rainfall extreme events, which often lead to floods or droughts. Both have been identified to exert significant impact on cultural, social, and economic life [*Schiermeier*, 2006; *Gadgil and Gadgil*, 2006; *Kshirsagar et al.*, 2006; *Sivakumar and Stefanski*, 2011; *Mirza*, 2011; *Turner and Annamalai*, 2012]. In recent years, several attempts have been made to understand and quantify the changes in the properties of extremes during the ISM in the context of global warming e.g., *Goswami et al.* [2006]; *Rajeevan et al.* [2008]; *Dash et al.* [2009]; *Krishnamurthy et al.*

[2009]; Ghosh et al. [2012]; Malik et al. [2010, 2012]; Singh et al. [2014]; Mishra and Liu [2014]. Several new insights about monsoonal changes were presented in these studies. For example, Goswami et al. [2006] and Rajeevan et al. [2008] concluded that ISM extreme rain events over central India are increasing. In contrast, Ghosh et al. [2012] concluded that there is no uniform spatial trend in extremes over the Indian subcontinent, but rather their variability is increasing. In a recent study by Singh et al. [2014] it has been shown that extreme wet and dry spells during the ISM have statistically significant changes in their intensity and frequency in the period between 1951 to 2011. Also, it has been suggested that the ISM is showing two contrasting phases: a wetter early summer followed by a drier period, with a possible influence of aerosol concentrations on precipitation patterns [Gautam et al., 2009; Kharol et al., 2013]. These changing rainfall patterns have been hypothesized to lead to an increased risk of droughts [Mishra and Liu, 2014]. See section S1 in the supporting information (SI) for further detailed discussion on ISM and climate change.

In our study, we present additional insights into the emerging features of the ISM rainfall over South and Southeast Asia by carrying out an analysis of two different climatic data sets: area-averaged time series of monthly rainfall from five different regions of India from 1871 to 2012 [Parthasarathy et al., 1993; Mooley et al., 1981; Parthasarathy et al., 1987], and gridded daily rainfall data for South and Southeast Asia from 1951–2007 [Yatagai et al., 2009]. This research differs from previous studies in the following critical ways: (1) We rely on a distinct computational method for trend analysis, known as *quantile regression*, which does not make any subjective choices on the rainfall amounts or return periods, as in more commonly used approaches involving linear regression and extreme value theory. *Quantile regression is an entirely different method from the common practice of using least squares linear regression for estimating trends in different quantiles.* (2) The majority of the previous studies used a data set that was limited to the political boundary of India. Instead, we analyze a data set with higher spatial resolution and larger spatial coverage, including all of South and Southeast Asia. Additionally, we have analyzed area-averaged time series extending from 1871 to 2012. (3) A large number of past studies have concentrated only on rain events related to high extremes, e.g., above the 90th percentile. Our study presents a more comprehensive analysis of extremes during the ISM and includes droughts as well. (4) Our results capture the regional variations of extremes. This is important because the ISM is composed of complex spatial patterns influenced by several local geographic factors such as topography and small-scale atmospheric processes.

2. Data and Method

In our study we rely on two data sets, the Homogeneous Indian Monthly Rainfall Data Set (1871–2012), a set of time series prepared by the Indian Institute of Tropical Meteorology hereafter referred to as IITM-HIMR [Mooley et al., 1981; Parthasarathy et al., 1987, 1993], and the gridded data set for the South Asia region from the APHRODITE (Asian Rainfall Highly Resolved Observational Data Integration Towards the Evaluation of Water Resources) project [Yatagai et al., 2009]. The APHRODITE data set (APHRO-V01003R1) includes spatial coverage for both South and Southeast Asia (see Fig. S1 for regions included in this analysis). For further details on the data set, including additional data sources, see section S2 of the SI.

We rely on quantile regression [Koenker and Hallock, 1978, 2001; Koenker, 2005], where one estimates the relationship between a variable X and conditional quantiles of response variable Y given that $X = x$, providing a more robust analysis of the central tendency and statistical dispersion of the relationship between variables. Conditional mean based classical (linear) regression is very sensitive to the extremes. In contrast, quantile regression is robust to the extremes of the response variable [Koenker and Hallock, 1978, 2001; Koenker, 2005], making it a much more powerful tool for studying trends of extremes in a distribution.

For a random sample of Y of size $n \{y_1, y_2, \dots, y_n\}$, in our data y_i is the rainfall on the x_i th day or year (depending on the temporal resolution of the data). We notate the cumulative distribution function by $F_Y(y) = P(Y \leq y)$. The τ th quantile of Y is given by $Q_Y(\tau) = \inf\{y : F_Y(y) \geq \tau\}$ where $\tau \in [0, 1]$. In this notation, $Q_Y(0.5)$ is the median of the sample Y .

Whereas one can obtain the sample mean of Y by minimizing a sum of squared residuals, the median can be obtained by minimizing a sum of absolute residuals $\min_{\xi \in \mathbb{R}} \sum_{i=1}^n |y_i - \xi|$. In general, one can obtain any other quantile by minimizing a sum of *asymmetrically* weighted absolute residuals, i.e., $\min_{\xi \in \mathbb{R}} \sum_{i=1}^n \rho_{\tau}(y_i - \xi)$ where ρ_{τ} is the tilted absolute value function, more specifically $\rho_{\tau}(z) = z(\tau - \mathbf{1}(z < 0))$, $\mathbf{1}(\cdot)$ denotes the indicator function. Quantile regression is specified in a form related to conditional expectation $E(Y|X = x)$, which can be estimated by $\hat{\beta} = \operatorname{argmin}_{\beta \in \mathbb{R}^p} \sum_{i=1}^n (y_i - \mu(x_i, \beta))^2$, where $\mu(x_i, \beta)$ is a parametric function. Instead, the conditional quantile functions are estimated by

$$\hat{\beta}(\tau) = \operatorname{argmin}_{\beta \in \mathbb{R}^p} \sum_{i=1}^n \rho_{\tau}(y_i - \xi(x_i, \beta)).$$

The function $\xi(x, \beta)$ is formulated as a linear function of the type $x_i^T \beta$. We have solved the above minimization problem by unconstrained nonlinear optimization, utilizing the *fminsearch* function available in the optimization toolbox of MATLAB®. The resulting quantities $\hat{\beta}(\tau)$ are called the *regression quantiles* [Koenker, 2005]. For linear quantile regression we will obtain two regression parameters from the quantile regression procedure: the intercept $\hat{\beta}_0(\tau)$ (rainfall magnitude at the initial time) and the slope of the fitted line $\hat{\beta}_1(\tau)$ (change in magnitude of rainfall per unit time). Rainfall in the x_i th year or day for the τ th quantile can then be estimated as $\hat{\beta}_0(\tau) + x_i \hat{\beta}_1(\tau)$.

To assess statistical significance, we construct the confidence interval of $\hat{\beta}(\tau)$ using a method of bootstrapping on residuals. This is accomplished by adding randomly resampled residuals back to the model fits to obtain synthetic samples of response variables. We generate 1000 such samples and employ the above described algorithm for quantile regression to estimate $\hat{\beta}_b^*$ ($b = 1, \dots, 1000$) on each of these synthetic samples of response variables. Next, we order $\hat{\beta}_1^* \leq \dots \leq \hat{\beta}_{1000}^*$ with the 95% confidence interval given by the 25th and 975th ordered elements. For significance testing, we reject the null hypothesis $H_0: \hat{\beta} = \hat{\beta}_0$ at the 5% significance level if $\hat{\beta}_0$ lies outside the above stated confidence interval.

For our purposes, extreme events are defined as the very low and very high quantiles of a distribution, following a convention that considers the top and bottom 10% as extremes [Field et al., 2014; Solomon et al., 2007]. We refer the reader to section S3 in the supporting information for details on the strength and limitations of quantile regression and section S3.1 for interpretation of trends and units used in the analysis.

3. Results

The IITM-HIMR data set (see section S2 of SI for the detailed description of the data set) provides area-averaged time series of monthly rainfall from 1871 to 2012 for five different regions of India: the regions are Northwest, Northeast, Peninsular, Central Northeast, West Central, and a sixth time series that is a composite of all regions, and is referred to as All India (see Fig. 1(a)). We have analyzed the time series individually to identify and compare trends in the annual JJAS rainfall in different regions of India. In Fig. 1(b–g) we show trends for different quantiles for all six time series, using quantile regression.

The threshold we have used for defining droughts is $\tau \in [0.1, 0.3]$, i.e., the bottom 10% ($\tau = 0.1$) to 30% ($\tau = 0.3$) annual rainfall amounts. These thresholds, highlighted by brown vertical bands in Fig. 1(b–g), are sufficiently low that they have the potential to cause drought conditions irrespective of other environmental conditions. Except Peninsular India, we observe intensification of droughts, i.e., decrease in rainfall intensity in $\tau \in [0.1, 0.3]$ quantiles in all of the other time series (West Central, Northeast, Central Northeast, Northwest and All India). In the four time series Northeast, Central Northeast, West Central and All India, we observe a decrease in the mean of the annual JJAS rainfall of 3 – 5% (see red dotted line in Fig. 1(b–g)).

In Fig. 1(b–g) we have highlighted higher quantiles, i.e., trends for $\tau \in [0.75, 0.95]$ by blue shaded vertical bands. Increase in these quantiles can indicate intensification of annual monsoonal rainfall. We observe that for the Northeast, Central Northeast and All India time series the rainfall appears to be mostly stable in these quantiles. Meanwhile, West Central and Northwest show some decrease in rainfall intensity in these quantiles. Although for some extremely low quantiles ($\tau < 0.1$) all regions except the Central Northeast show an increase in rainfall, it is difficult to draw definitive conclusions from these features as very few data points are available for such low quantiles in the 142 year annual time series.

For the Northwest region, we observe high variability in the trends for different quantiles (Fig. 1(f)). Lower quantiles show a massive decrease of up to 20%, while the moderate quantiles show an increase and higher quantiles show a decrease as well. The Peninsular region (Fig. 1(e)) shows a different trend compared to all the other regions, and it appears that rainfall is either increasing or stable across all quantiles. The All India time series also shows a decrease across all quantiles, close to the decrease in the mean rainfall. The two main results of our analyses are: (1) Rainfall is decreasing or stable to different degrees in all the regions except peninsular India where it has increased and (2) there is an intensification of droughts in the Northwest, Central Northeast, West Central and the Northeast.

To ascertain whether trends have shown any alterations over time, we have carried out further analysis of the six IITM-HIMR time series by estimating trends over moving time windows. We divide the time series into windows consisting of data points for 72 years with 67-year overlap between neighboring time windows (the total temporal range of each time series is 142 years) and estimate trends in two different quantiles ($\tau = 0.25$ characterizing droughts and $\tau = 0.85$ characterizing heavy rainfall) for each of these windows separately. Using this method of windowing we lose the ability to identify any alterations in trends before 1943 (the first window's end point). To quantify any gradual temporal shifts in trends of these quantiles, we estimate slopes of linear regression line fitted to data points from years before and after 1970. Negative (positive) signs of these slopes indicate gradual decrease (increase) in percentage trend for these two quantiles (see Fig. S2(b)). Although visual comparison gives the impression of a change point in 1970, a change-point analysis documents that none of these time series undergo a statistically-significant change point (Fig. S2c and explanation in the SI).

We observe a gradual change towards the intensification of droughts for all regions since 1970 (Fig. S2). Except for the Central Northeast, every region has experienced a gradual shift from less intense to more intense droughts. For the Northwest, the Central Northeast, the West Central, and All India we also observe decreasing strength of heavy monsoonal rainfall years since 1970 (Fig. S2(a)). These observations are indicative of some form of rainfall reduction over multiple parts of India. It has been hypothesized by *Bollasina et al.* [2011] that monsoonal precipitation over south Asia has decreased in the second half of the 20th century, due to the slowdown of the tropical meridional overturning circulation caused by increasing aerosol emissions over the region.

In order to enhance the spatial and temporal resolution of our analysis, we present the results of our analysis of the APHRO-V1003R1 data set (see section S2 of SI for the detailed description of the data set). This analysis is carried out at two different temporal resolutions: (i) total seasonal JJAS rainfall and (ii) daily rainfall during the JJAS season.

A decreasing trend in the lower quantiles ($\tau \leq 0.25$) of the seasonal JJAS rainfall documents intensification of drought situations at a grid point. The maximum intensification of droughts or strongest decrease in the lower quantiles of the annual JJAS rainfall are observed over parts of Myanmar, parts of Northwest India and adjoining parts of Central India (See Fig. 2(a–b) and Fig. S1). Other notable areas showing sharp intensification of droughts are the Northwest Himalaya and the high ISM rainfall zone west of the western Ghats (west coast of India along the Arabian Sea). Some parts of Eastern and Central India also show signs of intensification of droughts. An increasing trend in the higher quantiles ($\tau \geq 0.80$) of the annual JJAS rainfall will amount to above-average ISM rainfall for a grid point if the rainfall is evenly spread across four months of the JJAS season. If JJAS rainfall is not evenly distributed over the four ISM months then an increase may be associated with heavy rainfall events and related destruction of life and property. We observe an interesting pattern over parts of peninsular India with an increase in the higher quantiles of JJAS rainfall over almost the entire Indian peninsular, except over the western Ghats mountain range and regions west of them (a very high annual seasonal JJAS rainfall zone) (Fig. 2(c–d)). A similar increase can be observed over Eastern and Northeast India, Northern Myanmar. There is a general

decrease in annual ISM strength in the Himalaya and parts of Tibet, central Myanmar, parts of Central and Northwest India.

To detect changes in daily intense rainfall events in the APHRO–V1003R1 dataset, we analyze trends of the 0.995, 0.99, 0.975 and 0.95 quantiles (Fig. 3 a–d). These quantiles represent the top 0.5%, 1.0%, 2.5% and 5% of daily rain events, an increase in their intensity has the potential to cause large-scale flooding and may have large socio-economic impacts. These thresholds are chosen so that a particular extreme rain event (e.g., storm) does not make a trend, but rather a trend is estimated over multiple daily rainfall events across time. We observe a sharp increasing trend in Central India, parts of South India, South and Central Pakistan, parts of Northwest Himalaya and adjacent regions of Tibet for all of the above mentioned quantiles. In contrast, parts of Northwest India, Myanmar, Thailand and Cambodia show a rather strong decreasing trend in such events.

In an attempt to synthesize all of our findings, we have identified regions; with the most pronounced changes in extremes during the ISM season (Fig. 4). Through visual inspection of all our results (Fig. 1, 2, 3, S3 and S4), we have grouped spatially contiguous grid points with approximately similar trends into regions. We have delineated regions into two groups —regions with increase in the intensity of extreme daily rainfall and regions with intensification of droughts — because these will have the largest socio-economic impacts, as increasing strength of extreme rain events will increase chances of flash floods and increasing intensity of droughts can cause severe shortage of fresh water (additional details about steps followed in constructing Fig. 4 are provided in the SI Sec. S5). We have also listed some of the events (droughts or floods) within the identified regions, details about these events with corresponding references are provided in Table S1. Further discussion of results is provided in section S4.

4. Conclusion

Our study builds on previous analyses, but has added important methodological advantages, leading to the following key findings:

1. Decreasing trends in lower quantiles, generally associated with an intensification of droughts, is temporally the most stable and spatially the most extensive trend observed. Both data sets used in the analysis indicate that most of continental India shows a trend towards intensification of droughts. The regions of special concern in this context are Northwest India, parts of peninsular India and Himalaya, and all of Myanmar and some other parts of Southeast Asia (see a list of drought years in Table S2).
2. Analysis of the area-averaged monthly rainfall time series from 1871 to 2012 suggests that intensity of droughts has gradually increased since 1970. This drying could be related with increasing aerosol concentration over the region [*Bollasina et al., 2011*].
3. We have delineated regions which are most likely to be highly vulnerable to heavy rainfall events and related natural disasters, either due to increase

in the higher quantiles of annual JJAS rainfall or due to increase in the intensity of extreme rainfall events. Large parts of peninsular India and parts of eastern and central India show increasing trends in the higher quantiles of annual JJAS rainfall (top 20% years of JJAS rainfall). Also, there is a significant increase in extreme rain events especially at the top 1% over central India, Pakistan, parts of south and eastern India, and parts of Northwest Himalaya.

4. Apart from spatial inhomogeneity, we also observe dissimilarity in trends in different quantiles. For example parts of peninsular, central and eastern India show trends towards decreasing rainfall in lower quantiles, but also show increasing rainfall in the higher quantiles.
5. A spatially homogeneous trend of decreasing strength of moderate rainfall events (strongest 40% to 25% of rain events [Fig. S5 and S6]) seems to be emerging in the ISM area, even on time scales of just 6 decades. Similar observations have also been reported in previous studies [Goswami *et al.*, 2006; Rajeevan *et al.*, 2008; Dash *et al.*, 2009; Ghosh *et al.*, 2012]. In this study, we further unravel the spatial scale of this trend and show that it extends beyond continental India and covers almost all of South Asia. Furthermore, we found that this trend is more prominent in the regions of higher rainfall (wetter regions).

Our study suggests that the Indian Summer Monsoon region is a patchwork of trends with significant local and regional differences. Some regions are characterized by an increase in ISM rainfall, while other adjacent areas show an increase of droughts. The lack of a spatially-coherent trend of the Indian monsoon will require reassessment of the vulnerability and mitigation projections for this region. This study also demonstrates that the Indian monsoon system is responding in a complex fashion to global climatic forcing and that we do not anticipate to see homogeneous changes throughout the Indian monsoon domain.

Supplementary Material

Refer to Web version on PubMed Central for supplementary material.

Acknowledgments

The basic quantile regression code used in this work is based on the code written by Aslak Grinsted in MATLAB®, available to download from <http://www.mathworks.com/matlabcentral/fileexchange/32115>. Research reported in this publication was supported by the Eunice Kennedy Shriver National Institute of Child Health & Human Development of the National Institutes of Health under Award Number R01HD075712 and by Award Number R21GM099493 from the National Institute Of General Medical Sciences. The content is solely the responsibility of the authors and does not necessarily represent the official views of the National Institutes of Health.

References

- Bookhagen B. Appearance of extreme monsoonal rainfall events and their impact on erosion in the himalaya. *Geomatics, Natural Hazards and Risk*. 2010; 1(1):37–50. DOI: 10.1080/19475701003625737

- Bookhagen B, Burbank DW. Toward a complete himalayan hydrological budget: Spatiotemporal distribution of snowmelt and rainfall and their impact on river discharge. *Journal of Geophysical Research: Earth Surface*. 2010; 115(F3) n/a–n/a. doi: 10.1029/2009JF001426
- Bookhagen B, Thiede RC, Strecker MR. Abnormal monsoon years and their control on erosion and sediment flux in the high, arid northwest himalaya. *Earth and Planetary Science Letters*. 2005a; 231(12):131–146. <http://dx.doi.org/10.1016/j.epsl.2004.11.014>.
- Bookhagen B, Thiede RC, Strecker MR. Late quaternary intensified monsoon phases control landscape evolution in the northwest himalaya. *Geology*. 2005b; 33:149–152.
- Bollasina MA, Ming Y, Ramaswamy V. Anthropogenic Aerosols and the Weakening of the South Asian Summer Monsoon. *Science*. 2011; 334(502)
- Brakenridge, GR. Global active archive of large flood events. Dartmouth Flood Observatory, University of Colorado; <http://floodobservatory.colorado.edu/Archives/index.html>
- Carvalho LMV, Jones C, Silva AE, Liebmann B, Silva Dias PL. The south american monsoon system and the 1970s climate transition. *International Journal of Climatology*. 2011; 31(8):1248–1256. DOI: 10.1002/joc.2147
- Dash SK, Kulkarni MA, Mohanty UC, Prasad K. Changes in the characteristics of rain events in india. *J Geophys Res*. 2009; 114:D10, 109.
- Deser C, Phillips AS. Simulation of the 1976/77 climate transition over the north pacific: sensitivity to tropical forcing. *J Climate*. 2006; :6170–6180. DOI: 10.1175/JCLI3963.1
- Field, CB.; Barros, V.; Dokken, DJ.; Mach, KJ.; Mastrandrea, MD.; TEB, et al., editors. Contribution of Working Group I to the Fourth Assessment Report of the Intergovernmental Panel on Climate Change, 2007. Cambridge University Press; Cambridge, United Kingdom and New York, NY, USA: 2014.
- Gadgil S, Gadgil S. The indian monsoon, GDP and agriculture. *Econ PolitWeekly*. 2006; 41:4887–4895.
- Gadgil, S.; Kumar, K. The Asian Monsoon. In: Wang, B., editor. *The Asian monsoon - agriculture and economy*. Vol. chap 18. Springer; 2006.
- Gadgil S, Srinivasan J, Nanjundiah R, Kumar K, Munot AA, Kolli RK. On forecasting the indian summer monsoon: the intriguing season of 2002. *Curr Sci*. 2002; 83:394.
- Gautam R, Hsu NC, Lau K-M, Kafatos M. Aerosol and rainfall variability over the Indian monsoon region: distributions, trends and coupling. *Ann Geophys*. 2009; 27:3691–3703.
- Ghosh S, Das D, Kao S-C, Ganguly AR. Lack of uniform trends but increasing spatial variability in observed indian rainfall extremes. *Nature Climate Change*. 2012; 2
- Goswami BN, Venugopal V, Sengupta D, Madhusoodanan MS, Xavier PK. Increasing trend of extreme rain events over india in a warming environment. *Science*. 2006; 314:1442–1445. [PubMed: 17138899]
- Kala CP. Deluge, disaster and development in uttarakhand himalayan region of india: Challenges and lessons for disaster management. *International Journal of Disaster Risk Reduction*. 2014; 8(0): 143–152. <http://dx.doi.org/10.1016/j.ijdr.2014.03.002>.
- Kharol SK, Kaskaoutis DG, Sharma AR, Singh RP. Long-Term (1951–2007) Rainfall Trends around Six Indian Cities: Current State, Meteorological, and Urban Dynamics. *Advances in Meteorology*. 2013; 2013:572954.
- Koenker, R. *Quantile Regression*. Cambridge University Press; 2005.
- Koenker R, Hallock KF. Regression quantiles. *Econometrica*. 1978; 46:33–50.
- Koenker R, Hallock KF. Quantile regression. *Journal of Economic Perspectives*. 2001; 15(4):143–156.
- Krishnamurthy CKB, Lall U, Kwon H-H. Changing frequency and intensity of rainfall extremes over india from 1951 to 2003. *J Clim*. 2009; 22:4737–4746.
- Kshirsagar N, Shinde R, Mehta S. Floods in Mumbai: Impact of public health service by hospital staff and medical students. *Journal of Postgraduate Medicine*. 2006; 52(4):312–314. [PubMed: 17102558]
- Kumar A, Dudhia J, Rotunno R, Niyogi D, Mohanty UC. Analysis of the 26 july 2005 heavy rain event over mumbai, india using the weather research and forecasting (wrf) model. *Q J R Meteorol Soc*. 2008; 134:1897–1910.

- Kumar KK, Rajagopalan B, Hoerling M, Bates G, Cane M. Unravelling the mystery of indian monsoon failure during elnino. *Science*. 2006; 314:1131, 152.
- Kumar KN, Rajeevan M, Pai DS, Srivastava A, Preethi B. On the observed variability of monsoon droughts over india. *Weather and Climate Extremes*. 2013; 1:42–50.
- Malik N, Marwan N, Kurths J. Spatial structures and directionalities in monsoonal precipitation over south asia. *Nonlinear Processes in Geophysics*. 2010; 17(5):371–381. DOI: 10.5194/npg-17-371-2010
- Malik N, Bookhagen B, Marwan N, Kurths J. Analysis of spatial and temporal extreme monsoonal rainfall over south asia using complex networks. *Climate Dynamics*. 2012; 39(3–4):971–987. DOI: 10.1007/s00382-011-1156-4
- Marengo JA. Interdecadal variability and trends of rainfall across the amazon basin. *Theoretical and Applied Climatology*. 2004; 78(1–3):79–96. DOI: 10.1007/s00704-004-0045-8
- Mirza MMQ. Climate change, flooding in south asia and implications. *Reg Environ Change*. 2011; 11(Suppl 1):S95–S107.
- Mishra A, Liu SC. Changes in precipitation pattern and risk of drought over india in the context of global warming. *Journal of Geophysical Research: Atmospheres*. 2014; 119(13):7833–7841. DOI: 10.1002/2014JD021471
- Mooley DA, Parthasarathy B, Sontakke NA, Munot AA. Annual rain-water over india, its variability and impact on the economy. *J Climatol*. 1981; 1:167–186.
- Nagarajan, R. *Drought Assessment*. Springer; 2009.
- Parthasarathy B, Sontakke NA, Munot AA, Kothawale DR. Droughts/floods in the summer monsoon rainfall season over different meteorological subdivisions of india for the period 1871–1984. *J Climatol*. 1987; 7:57–70.
- Parthasarathy B, Kumar KR, Munot AA. Homogeneous indian monsoon rainfall : variability and prediction. *Proc Indian Acad Sci (Earth Planet Sci)*. 1993:121–155.
- Rajeevan M, Bhate J, Jaswal AK. Analysis of variability and trends of extreme rainfall events over india using 104 years of gridded daily rainfall data. *Geophys Res Lett*. 2008; 35(18)doi: 10.1029/2008GL035143
- Schiermeier, Q. Extreme monsoons on the rise in india. *Nature*. 2006. <http://dx.doi.org/10.1038/news061127-12>
- Singh D, Tsiang M, Rajaratnam B, Diffenbaugh NS. Observed changes in extreme wet and dry spells during the south asian summer monsoon season. *Nature Clim Change*. 2014; 4:456–461.
- Sivakumar, MVK.; Stefanski, R. *Climate Change and Food Security in South Asia*. In: Lal, R.; Sivakumar, MVK.; Faiz, SMA.; Rahman, AHMM.; Islam, KR., editors. *Climate Change in South Asia*. Vol. chap 2. Springer; 2011.
- Solomon, S.; Qin, D.; Manning, M.; Chen, Z.; Marquis, M.; Averyt, K.; Tignor, M.; Miller, H., editors. *Climate Change 2014: Impacts, Adaptation, and Vulnerability Part A: Global and Sectoral Aspects*. Cambridge University Press; Cambridge, United Kingdom and New York, NY, USA: 2007.
- Turner A, Annamalai H. Climate change and the south asian summer monsoon. *Nature Climate Change*. 2012; 2:587–595.
- Wang, B., editor. *The Asian Monsoon*. Springer; 2006.
- Wang P, Clemens S, Beaufort L, Braconnot P, Ganssen G, Jian Z, Kershaw P, Sarnthein M. Evolution and variability of the asian monsoon system: state of the art and outstanding issues. *Quat Sci Rev*. 2005; 24:595–629.
- Webster PJ, Magana VO, Palmer T, Shukla J, Tomas RA, Yani M, Yasunari T. Monsoons: processes, predictability, and the prospects for prediction. *Journal of Geophysical Research*. 1998a; 103:14,451–14,510.
- Webster PJ, Toma VE, Kim HM. Were the 2010 pakistan floods predictable? *Geophys Res Lett*. 2011; 38:L04806.
- Wulf H, Bookhagen B, Scherler D. Climatic and geologic controls on suspended sediment flux in the sutlej river valley, western himalaya. *Hydrology and Earth System Sciences*. 2012; 16(7):2193–2217. DOI: 10.5194/hess-16-2193-2012

Yatagai A, Arakawa O, Kamiguchi K, Kawamoto H. A 44 year daily gridded precipitation dataset for asia based on dense network of rain gauges. SOLA. 2009; 5:137–140.

Author Manuscript

Author Manuscript

Author Manuscript

Author Manuscript

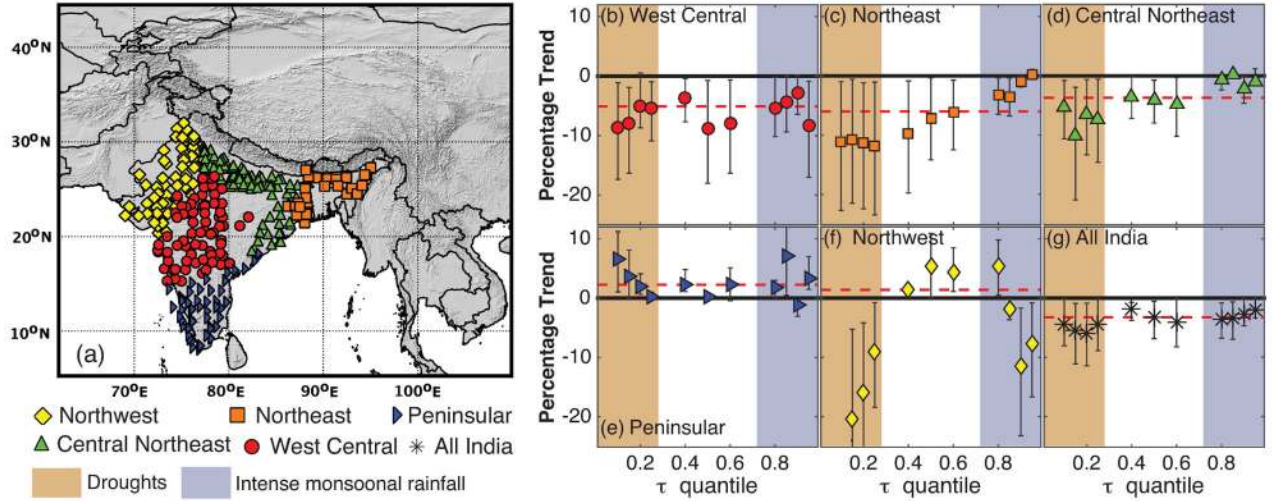


Figure 1.

(a) Station locations used in the constructing of area-averaged time series of the IITM-HIMR data set (1871–2012), for different homogeneous rainfall regions. Each color represents one particular region, whereas ‘All India data’ includes all stations. IITM-HIMR data consists of area averaged monthly rainfall amounts from 1871 to 2012. We have built the time series of annual ISM rainfall from these data by taking the average over JJAS months for each year. (b)–(g) Markers are the percentage trend in each quantile over the 142 year period, marker colors and shape correspond to different geographic regions and the error bars represent the 95% confidence intervals obtained using method of bootstrapping on residuals. Red dotted lines indicate the linear trend in the mean of the respective time series over the 142 years, independent of quantiles. Black heavy lines act as a reference for no change/no trend. Quantile values are indicated by τ (horizontal axes). Brown-shaded vertical bands highlight the lower quantiles i.e., trends for $\tau \in [0.1, 0.3]$. Blue-shaded vertical bands highlight the higher quantiles, i.e., trends for $\tau \in [0.75, 0.95]$. Observe the low values of the quantile trends for $\tau \in [0.1, 0.3]$ for West Central, Central Northeast, Northeast, Northwest, and All India indicating intensification of droughts in these regions. See Figs. S7, S8 and S9 and Sec. S3.2 for additional information.

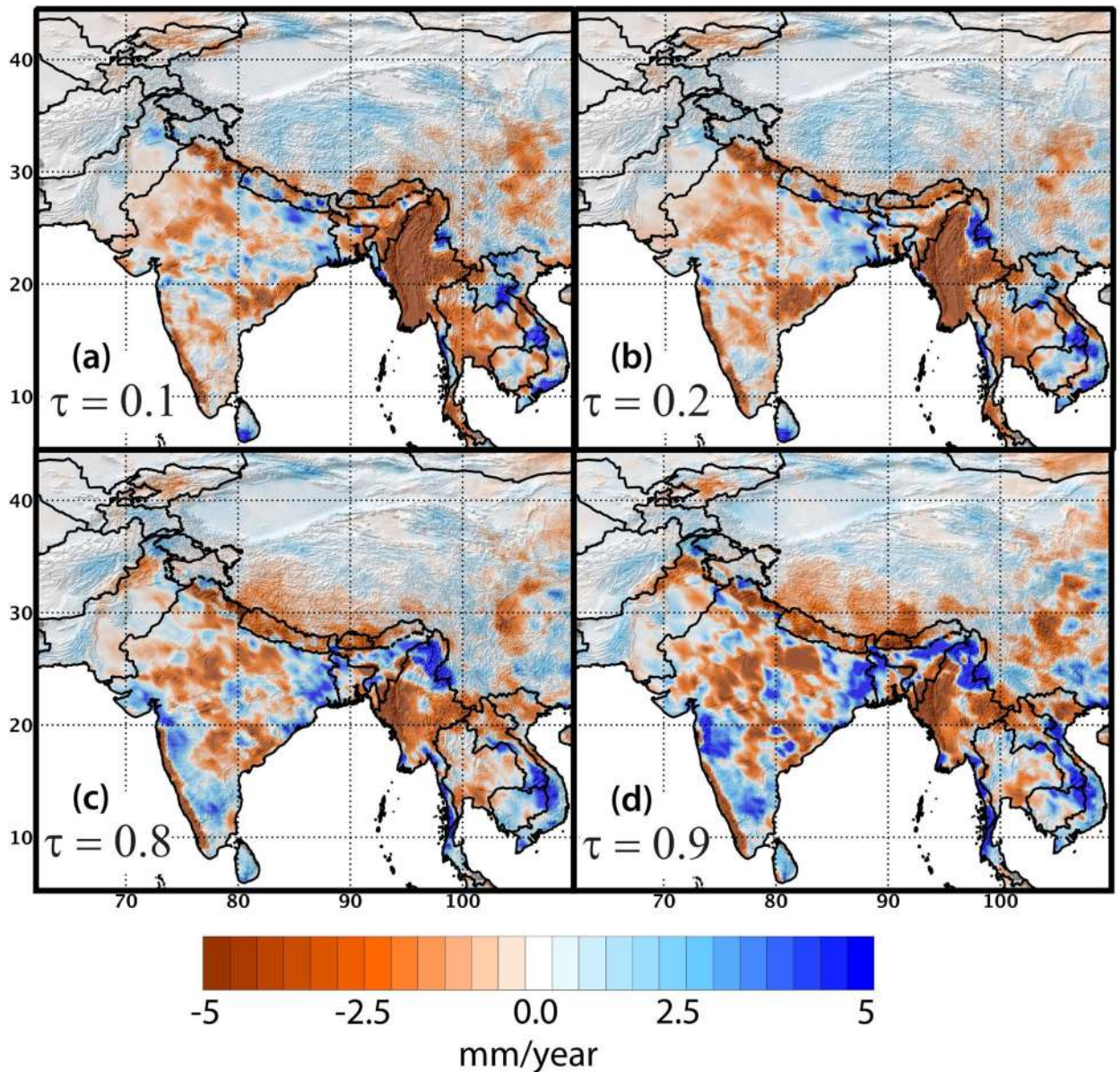


Figure 2.

Trends in the *annual JJAS* rainfall based on the analysis of the spatial gridded APHRO-V1003R1 data set (1951–2007). Annual JJAS rainfall amounts (in *mm*) at a grid point were calculated by summing daily rainfall amounts of 122 JJAS days. Trend in the (a) 10th and (b) 20th percentile of the annual JJAS rainfall. A negative trend indicates a decrease in rainfall for these quantiles and can be associated with an intensification of droughts. Trend in the (c) 80th and (d) 90th percentile of the annual JJAS rainfall. A positive trend indicates an increase in rainfall for these quantiles which may be associated with a higher frequency and/or greater strength of intense rainfall events. To obtain net increase in *mm* over the entire time period of the data set (1951–2007), multiply the value given above in *mm/year* by 56. For further details about converting and interpreting above units for trends see section S3.1. For comparison with other τ thresholds and data sets see Figs. S3 and S4.

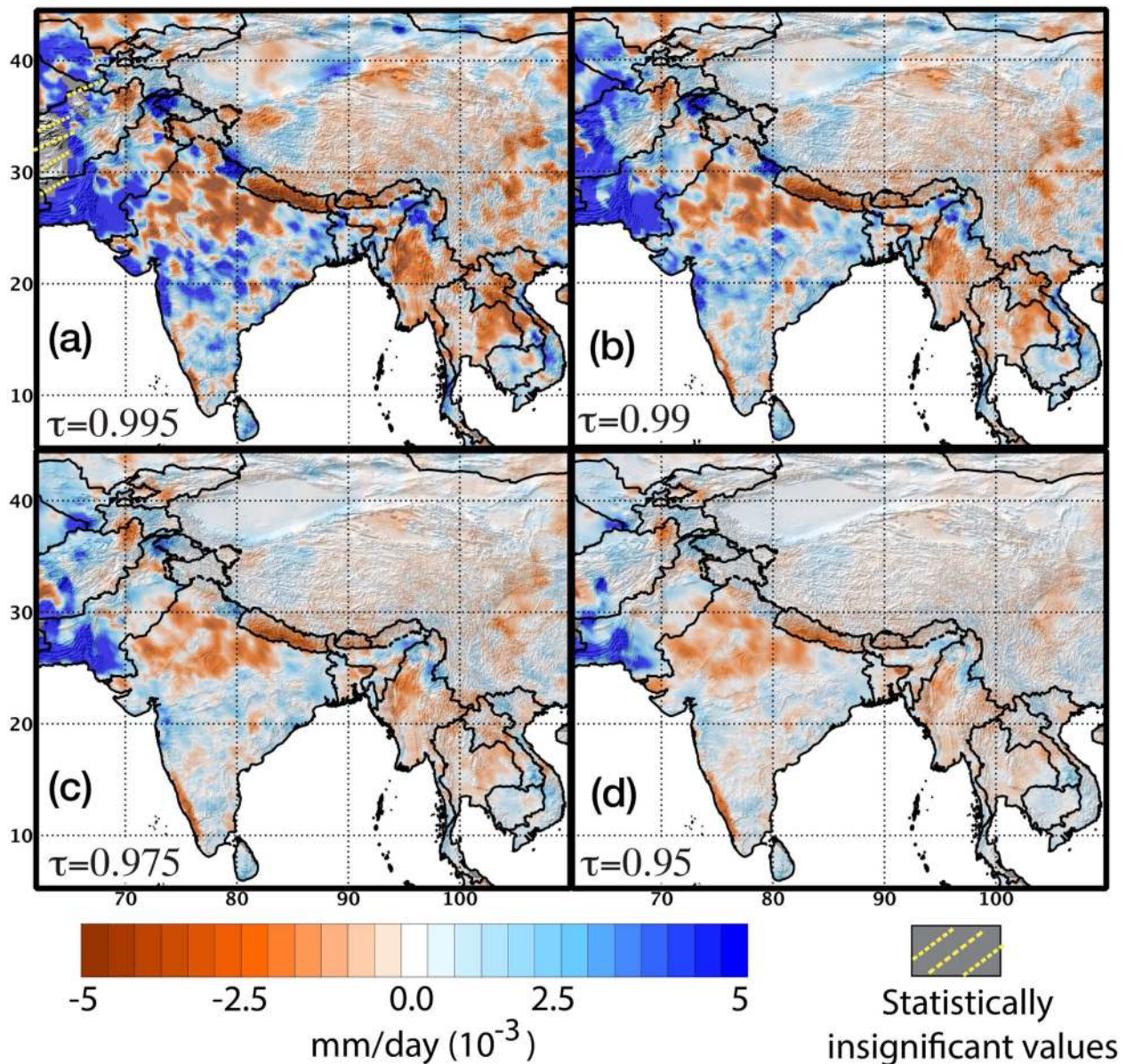


Figure 3.

Trends in the extreme *daily* JJAS rainfall events based on the analysis of the spatial gridded APHRO-V1003R1 data set (1951–2007). The unit of daily rainfall in this data set is *mm*, and for the analysis we have used all the JJAS days (6954) available in the data set. Trend in the (a) 99.5th, (b) 99th, (c) 97.5th and (d) 95th percentile of the daily rain events during JJAS. An increase of intense rainfall events has the potential to lead to flash floods and associated hazards. Observe the increasing trend over parts of south Pakistan, and the Northwest and Karakoram Himalaya. Trend increases can also be seen in central and eastern India and the northeast Himalaya. Baseline magnitudes (intercepts of the fitted lines) for these thresholds are available in Fig. S14. To obtain net increase in *mm* over the entire time period of the data set (1951–2007), multiply the value given above in *mm/day* by 6953, i.e.,

one less than the total number of JJAS days in the data. See section S3.1 for converting and interpreting above units for trends.

Author Manuscript

Author Manuscript

Author Manuscript

Author Manuscript

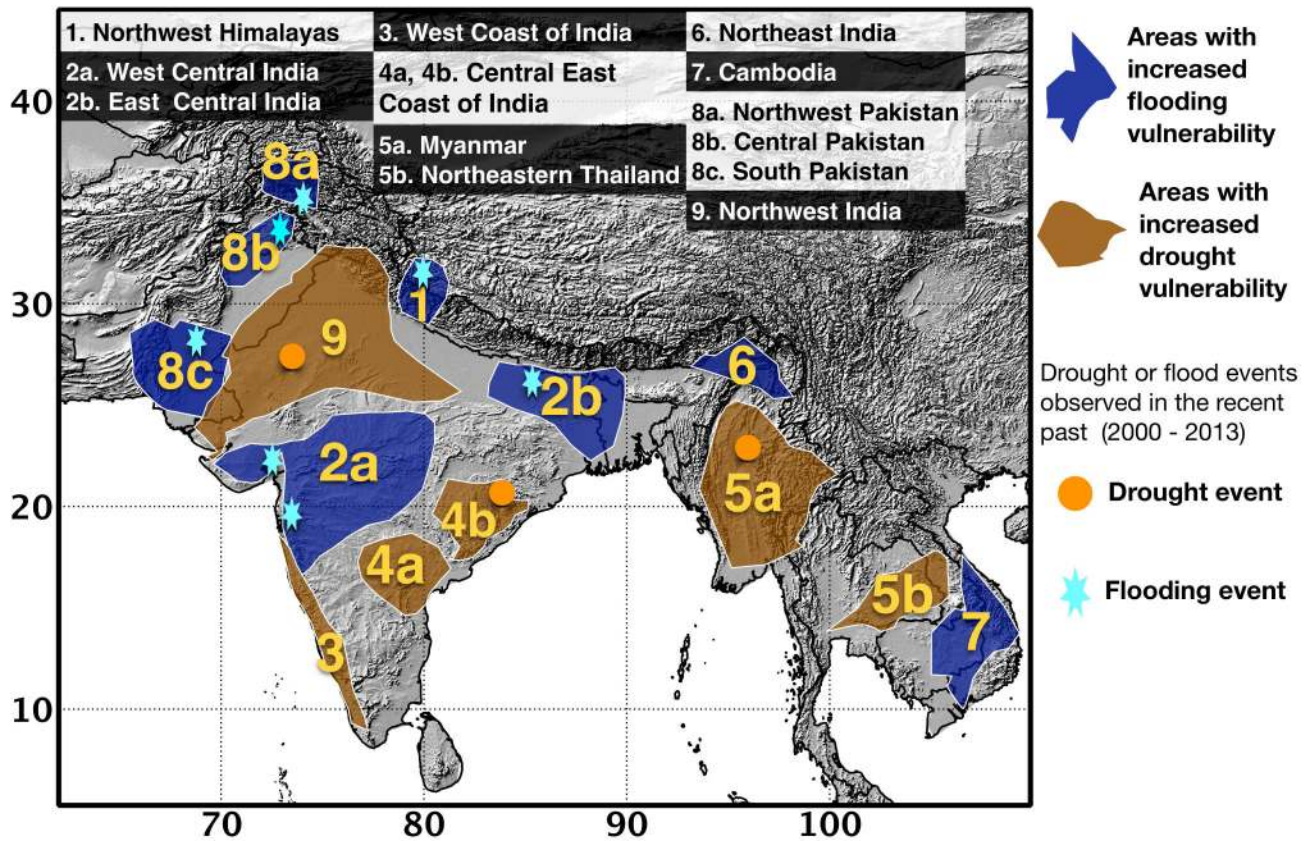


Figure 4.

Synthesis showing spatial patterns of strongest rainfall trends in the extremes during the ISM season over the past 57 years. Brown regions indicate increasing trends in lower quantiles, often associated with drought conditions, while blue regions indicate areas with increasing rainfall at the higher percentiles, generally characterized by an increase in flooding. Region numbers and associated geographic regions are shown on the right. The demarcation of drought regions has also been corroborated by our observed trends (Fig. 1). We use light blue (flood) stars and orange (droughts) dots to indicate particular events during the recent past (between the years 2000 to 2013). These events were either extensively studied by the scientific community or have been reported by international media coverage (see SI material Table S1, Fig. S12, S13 and Sec. S5 for additional information).